[AMERICAN JOURNAL OF SCIENCE, VOL. 287, JUNE, 1987, P. 612-634]

ANALYSIS OF BUCKLE FOLDS FROM THE EARLY PROTEROZOIC OF MINNESOTA

TIMOTHY B. HOLST
University of Minnesota, Duluth, Duluth, Minnesota 55812

ABSTRACT. A series of minor folds exists in the early Proterozoic Little Falls Formation in Central Minnesota. The folds are developed in thin (up to 2 cm) quartz layers embedded in slate. The slate has a single, well-developed cleavage, and the rocks have been metamorphosed to lower amphibolite facies. Axial surfaces of the folds are vertical, and fold axes are subhorizontal. The folds exhibit geometries ranging from class 1B (parallel) to class 1C and are interpreted as buckle folds which have undergone a small amount of late-stage flattening. Arclength/thickness data (measured perpendicular to the fold hinge) were collected from 343 quarter-arc fold segments from 31 "fold trains." The mean arclength/thickness ratio is 6.2, with a dispersion of 0.36. The presence of deformed concretions allows the determination of finite strain in the slate matrix, with X:Y:Z = 6.3:3.5:1. Reasonable estimates of volume loss during deformation then suggest that the layer-parallel shortening in the buckled layer during the buckling (wavelength selection) process was in the range of 40 to 50 percent. Although these data do not constrain exactly the interpretation, buckling theory suggests the quartz layers followed a flow law with a value of n between 1 and 2, with layer/matrix effective viscosity ratio in the range 20 to 40, and amplification in the range 20 to a few hundred.

INTRODUCTION

During the past several decades our understanding of the buckling process in both Newtonian (linear viscous) and non-linear materials has greatly increased. This has been accomplished through theoretical studies (for example, Biot, 1961; Ramberg, 1961; Sherwin and Chapple, 1968; Fletcher, 1974; Smith, 1975, 1977, 1979) as well as experimental studies (for example, Biot, Ode, and Rover, 1961; Agostino, 1971; Hudleston, 1973a; Cobbold, 1975; Manz and Wickham, 1978; Neurath and Smith, 1982) and numerical modelling (for example, Chapple, 1968; Dieterich, 1969; Parrish, 1973; Hudleston and Stephansson, 1973; Fletcher and Sherwin, 1978). These studies have resulted in a set of parameters that can be used to interpret the nature of the folding and the rheological properties of the materials during the buckling process for naturally-occurring folds. The most useful parameters are the fold shape on a hinge-perpendicular section, the frequency distribution of arclength/thickness ratios (L) for a fold population, and the strain distribution. Especially important is the amount of layer-parallel shortening (T) that took place within the folded layer during the buckling process. Unfortunately not all the pertinent parameters may be measured in most natural geologic situations, and interpretations of data on geometry and strain distribution in natural folds by application of buckling theory are relatively few (for example, Sherwin and Chapple, 1968; Hudleston, 1973b; Fletcher, 1974;

Smith, 1979; Hudleston and Holst, 1984). In the present study, although not all the parameters may be specified exactly, the quantities may be sufficiently constrained for a buckling analysis to be carried out.

GEOLOGIC SETTING

Stratigraphy.—The early Proterozoic Little Falls Formation is a series of graywackes and slates which are fairly poorly exposed in central Minnesota (fig. 1). It is part of a thick sequence of early Proterozoic supracrustal rocks which are fairly widespread in the Great Lakes region of North America, and which also contain the Lake Superior-type banded iron formations. The Little Falls Formation has been assigned to the Mille Lacs Group, the lower of two formal stratigraphic groups of early Proterozoic supracrustal rocks in the region (Morey, 1978), although stratigraphic relationships in the area have recently been re-evaluated (Morey and Southwick, 1984). To the north on the Mesabi Iron Range,

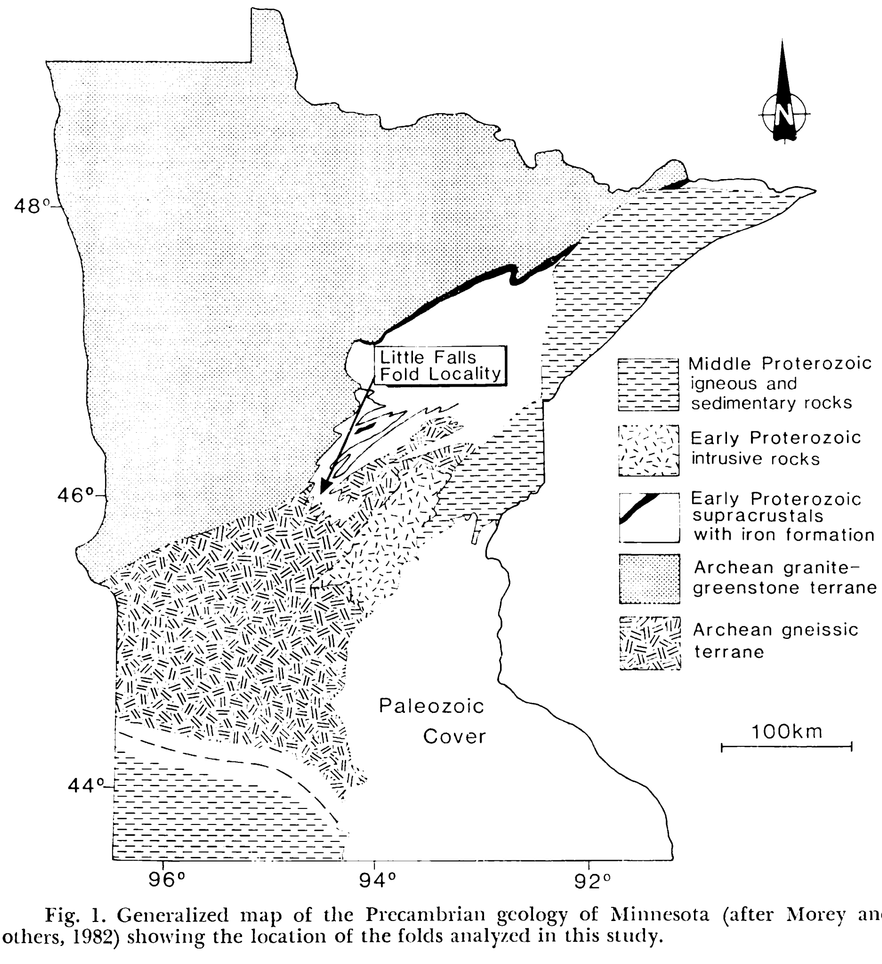

Fig. 1. Generalized map of the Precambrian geology of Minnesota (after Morey and others, 1982) showing the location of the folds analyzed in this study.

these early Proterozoic suprcrustal rocks may be observed to overlie unconformably rocks of an Archean granite-greenstone belt terrane (2750-2600 my, Morey and others, 1982). In central Minnesota the supracrustal rocks are cut by Penokean granites (1850-1800 my, Morey and others, 1982), and to the east they are cut and overlain by igneous and sedimentary rocks of middle Proterozoic (Keweenawan) age (1140 my, Morey and others, 1982).

Structural geology and tectonic setting.—At the type locality of the Little Falls Formation, there is a single fold generation present, with wavelengths of folds from centimeters to at least several tens of meters. The folds are open, upright, and sub-horizontal. Axial-surface strikes and fold-axis trends are within a few degrees of 030. There is a single, sub-vertical, well-developed slaty cleavage which is axial-planar to the folds. The rocks have been metamorphosed to lower amphibolite facies (Morey, 1980). In one area at the type locality, there is a series of small quartz veins embedded in the slate. Where bedding in the matrix can be observed, the quartz layers and bedding are parallel. Small folds possessing characteristics of buckle folds exist in the quartz layers, particularly in one area of outcrop. Vertical joint surfaces perpendicular to the cleavage provide good hinge-perpendicular surfaces for fold observation. Cleavage surfaces allow inspection in the third dimension. These small folds, the object of this study, will be described in detail in a later section.

The early Proterozoic supracrustal rocks of central Minnesota (fig. 1) were deformed, along with rocks farther to the east in Minnesota, Wisconsin, and Upper Michigan, during the Penokean orogeny (1875-1825 my, Van Schmus, 1976, 1980). In east-central Minnesota, where exposure of deformed early Proterozoic supracrustal rocks is better than in the Little Falls area, two structural terranes have been defined (Holst, 1982a, 1984, 1985a,b). The southern terrane suffered two main phases of Penokean deformation, the earlier involved large-scale recumbent structures and the later upright, sub-horizontal, open folds. There is a well-developed, early, bedding-parallel foliation, and a later, sub-vertical spaced crenulation cleavage. The northern terrane was involved in only the second deformation and has a single, sub-vertical, well-developed slaty cleavage in addition to the upright folds. The structural features present at the type locality of the Little Falls Formation are very similar to the northern terrane in east-central Minnesota and are most simply interpreted as having suffered a single deformational event. However, geophysical trends (Chandler, Nordstrand, and Anderson, 1984) indicate the southern, multiply-deformed terrane of east-central Minnesota does extend into central Minnesota (Morey and Southwick, 1984), and examination of drill core in central Minnesota has revealed a number of areas of early Proterozoic rocks with two well-developed cleavages (Southwick, personal commun.).

FOLD DESCRIPTION AND GEOMETRY

The small-scale folds developed in the thin (up to 2 cm) quartz layers show many of the features typical of buckle folds. The orthogonal thickness of the layers is fairly constant around the folds, and there is a preferred arclength which is dependent on layer thickness. Where bedding in the slate matrix is visible, the folds die out rapidly above and below the quartz layers into the slate matrix. Some of the folds in the quartz layers are symmetric, but others, on the limbs of larger-scale folds in the slate (wavelengths of several meters), are asymmetric and show normal vergence relationships to the larger folds. Axial surfaces of the folds in the quartz layers are sub-vertical and parallel to the slaty cleavage in the matrix. Fold axes are within a few degrees of horizontal. Most of the folded quartz layers are sufficiently far apart so that it is clear they were behaving as isolated single layers during buckling. Those that are close to one another, or that have layer-parallel slaty inclusions, may have acted as multi-layers during deformation and were not used in this study. Drawings of five of the fold trains from which data were collected for this study are shown in figure 2.

Fold geometries are parallel or sub-parallel, that is of class 1B or class 1C (Ramsay, 1967). Figure 3 shows a $t'\alpha$ diagram with exact plots for 14 representative fold limbs. Five of the fold limbs are of precisely constant orthogonal thickness (perfect parallel, class 1B folds), while nine fall just into the 1C fold class.

For buckling analysis the distribution of arclength/thickness ratios is of particular interest. Photographs of the folds were taken in the field, with care taken that the camera film plane was perpendicular to the fold hinge. Enlargements of these photos were taken back into the field where exact boundaries of layer/matrix contacts were drawn on the photographic enlargements. The distance along the middle of a layer, from a

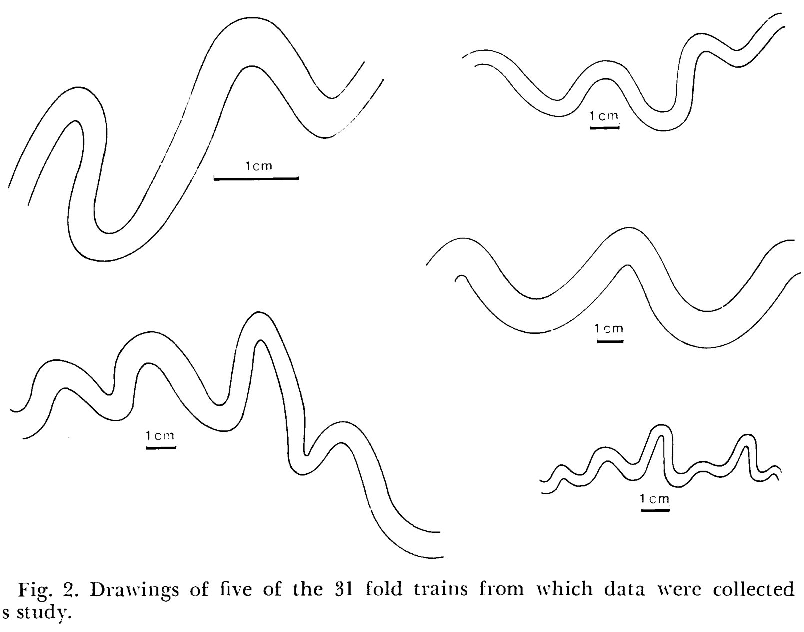

Fig. 2. Drawings of five of the 31 fold trains from which data were collected for this study.

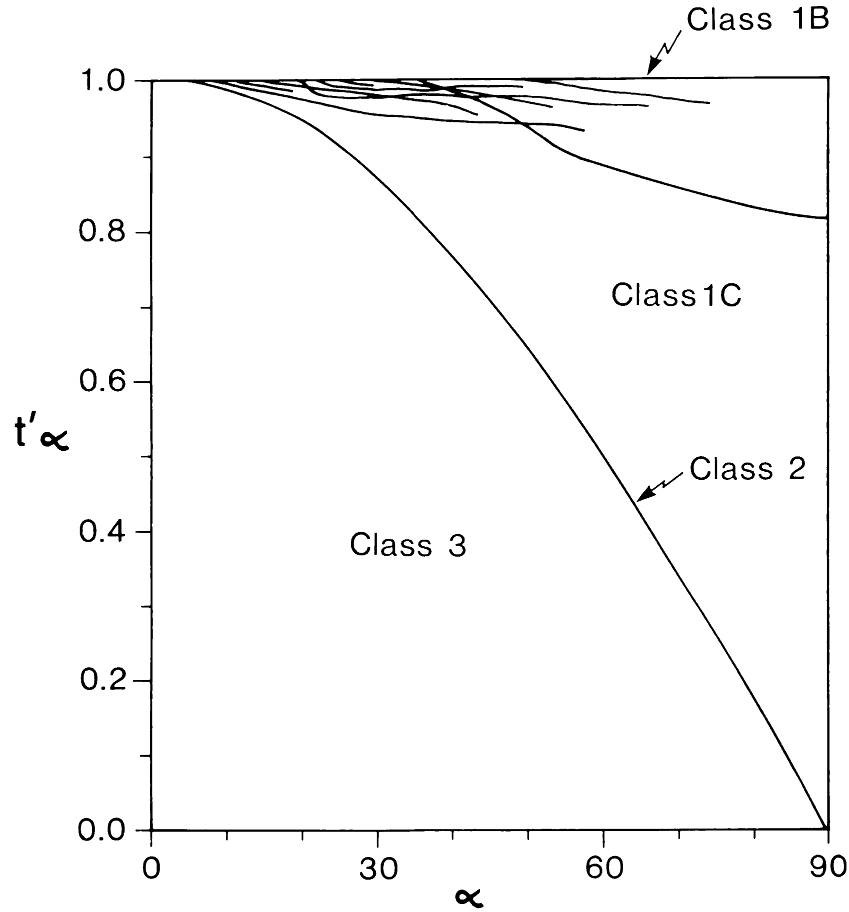

Fig. 3. t′α plot for 14 selected fold limbs. Of the fourteen limbs, five are class 1B (parallel) folds and plot along the line at the top of the diagram.

fold hinge to the inflection point is the arclength of a quarter-arc segment of a fold. This distance was determined for 343 quarter-arc fold segments, from 31 fold trains. Along each quarter-arc segment, the orthogonal thickness of the layer was measured from at least three places. These measurements were made directly from the annotated photographic enlargements with the aid of a digitizing pad and a microcomputer. The arclength/thickness ratio for a full wavelength, L (4 times the arclength/thickness ratio for each quarter-arc segment), was then calculated. The frequency distribution of L is shown in figure 4. The mean arclength/thickness ratio ($\bar{L}$) for the fold population is 6.2, with a standard deviation of 3.2.

FINITE STRAIN MEASUREMENTS IN THE MATRIX

Strain markers.—Deformed carbonate concretions are present in the Little Falls Formation at the type locality and in exposures in the sur-

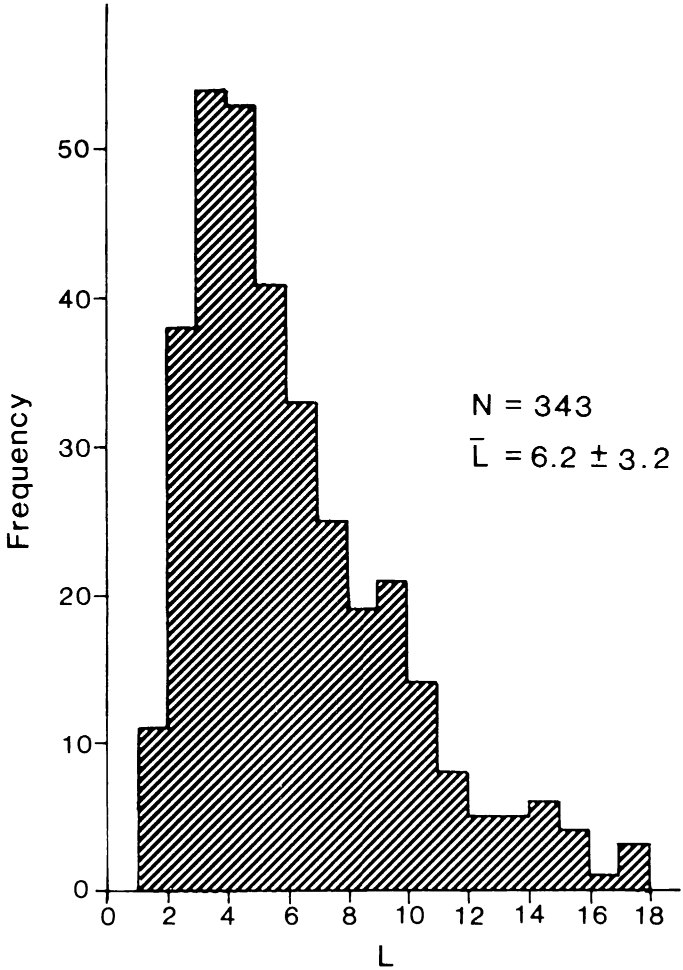

Fig. 4. Histogram of L, the ratio of one full arclength to average layer thickness, for the 343 quarter-arc segments analyzed. The mean value ($\bar{L}$) is 6.2, with a standard deviation of 3.2.

rounding area. They are similar to deformed concretions found in other early Proterozoic graywacke-slate units in Minnesota (Schwartz, 1942; Morey and Ojakangas, 1970), which have also been used for finite strain analysis (Holst, 1985a). In that study (Holst, 1985a) it was found that similar strain results were obtained using deformed concretions, mud chips, and conglomerate clasts as strain markers.

Strain measurement techniques.—The shape and orientation of deformed concretions on two-dimensional outcrop surfaces were recorded in the field. These data were plotted on standard ln R_f-ϕ plots (Ramsay, 1967; Dunnet and Siddans, 1971) and on the polar plot (Elliott, 1970;

Holst, 1982b), for two-dimensional strain determination. Three-dimensional strain was calculated using two-dimensional data from three different surfaces. To gather sufficient concretion shape data, outcrops within several hundred meters of the fold outcrop were used. Details of the strain measurement techniques may be found in Holst (1985a).

Results.—The analysis of deformed concretions reveals that the strain ellipsoid in the slate matrix has a ratio of principal strains of 6.3:3.5:1 (X:Y:Z = 6.3:3.5:1, X>Y>Z). This value is plotted as an x on figures 5A and 5B. This ellipsoid lies well within the flattening field (X>Y>>Z) for no volume change. As shown on figure 5, this result is in general agreement with adjacent areas with apparently similar structural histories. The box on figure 5 is the strain ellipsoid obtained from a deformed conglomerate 17 km northwest of the fold locality. The circles are results from deformed concretions, mud chips, and conglomerates 170 km to the northeast (Holst, 1985a). In each of these areas there are open, upright, sub-horizontal folds and a single, well-developed sub-vertical axial-planar cleavage. The Little Falls Formation strain result is also well within the field defined by 5200 strain determinations in slates (Wood, 1974). The maximum extension (X) in the Little Falls Formation is vertical (sub-orthogonal to fold axes), and the maximum shortening (Z) is horizontal, perpendicular to the axial-planar slaty cleavage (fig. 6). This is also the geometry commonly found in slates by Wood (1974).

Volume loss considerations.—The result produced by a strain analysis using deformed markers such as in this study is a ratio of principal strain values and the orientation in space of the three principal axes. Actual values of extension in any direction may be calculated only when a particular volume change during deformation is assumed. Volume change and deformation has been considered in some detail by Ramsay and Wood (1973), and Wood (1974) suggested that most slates have undergone some volume loss during the deformation process and development of slaty cleavage. Figure 5B shows lines of plane strain (Y=1) for various values of volume loss.

Wright and Platt (1982) were able to measure actual extensions in particular directions within the deformed Martinsburg shale of the Appalachian Mountains by the use of deformed graptolites whose undeformed dimensions are known. They were able to show that their measurements were consistent with a 50 percent volume loss and not compatible with a constant-volume deformation. In that particular case, *no* extension was found within the cleavage plane, and shortening of 50 to 70 percent was found at high angles to cleavage, so that the shape of the finite strain ellipsoid was also consistent with the findings of Wood (1974) for slates in general.

For the slates of the Little Falls Formation, as in most rocks, no specific information on volume change is available. That is, it is not possible to measure exact finite extensions in any direction. Evidence of pressure solution perpendicular to the cleavage is commonly seen in thin section, and some volume loss could easily have occurred during the

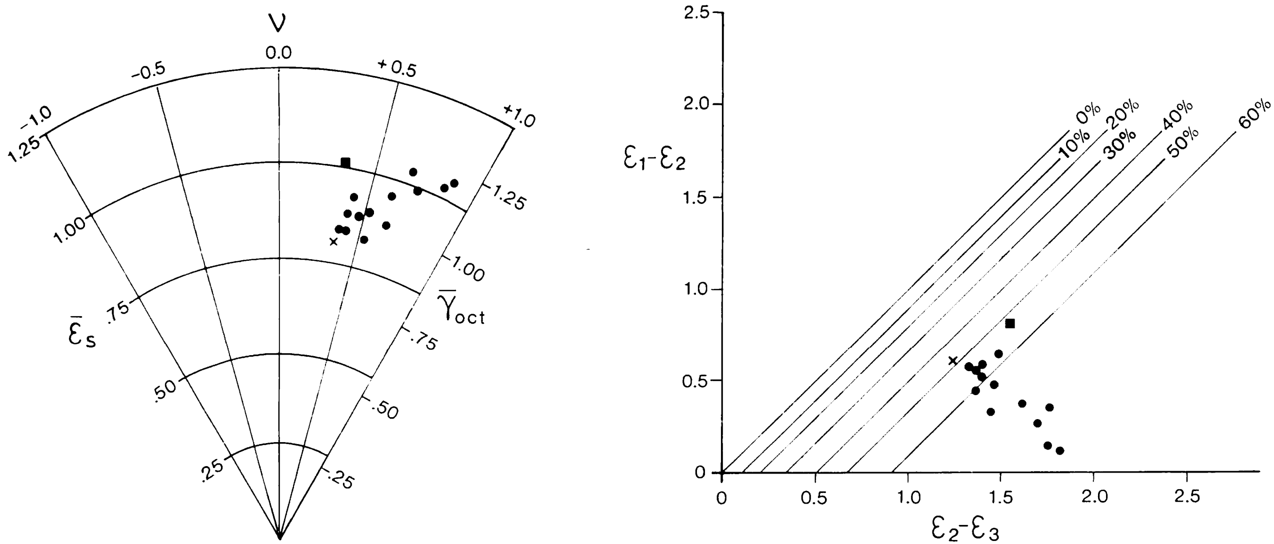

Fig. 5. Results of three-dimensional strain determinations in Little Falls Formation (x), Randall Formation (box), and 13 localities in the northern terrane of the Thomson Formation (dots). (A) plot of the strain parameter $\bar{\varepsilon}_s$ versus Lode's parameter, ν (see Hossack, 1968). Also shown are values of $\bar{\gamma}_{oct}$, the natural octahedral unit shear (Nadai, 1963). (B) Logarithmic deformation plot (Ramsay, 1967) of same data as A. The lines are loci of plane strain (Y=1) for the labelled amounts of volume loss.

geneous flattening, but a comparison of figure 3 with the calculations of Ramsay (1967, fig. 7-79, p. 413) for flattened parallel folds shows that an average value of late-stage flattening for the folds in this study is at most a few (<5) percent. The buckle shortening was calculated for the 31 fold trains studied, with results shown in figure 7. If we take $(1+e)_b$ in eq 1 as the mean value measured in this way (0.63), for a given estimate of volume loss it will be possible to calculate $(1+e)_{tot}$; and then $(1+e)_{l.p.s.}$, critical to the buckling analysis, may be calculated. This was done for volume loss estimates from 0 to greater than 90 percent, and the results are shown graphically in figure 8. The estimate of layer-parallel shortening during the buckling process for the folds in this study is seen to be relatively insensitive to volume loss for reasonable values of volume loss. For example at no volume loss, layer-parallel shortening is estimated to be 42 percent, and at 40 percent volume loss, layer-parallel shortening is estimated to be 52 percent. Thus it seems reasonable to suggest that layer-parallel shortening during the buckling process for these folds was in the range of 40 to 50 percent ($2.8 \leq T \leq 4$). This is similar to the amounts of the layer-parallel shortening seen in buckling experiments using linear-viscous materials at low (<100) viscosity contrasts (Hudleston, 1973a).

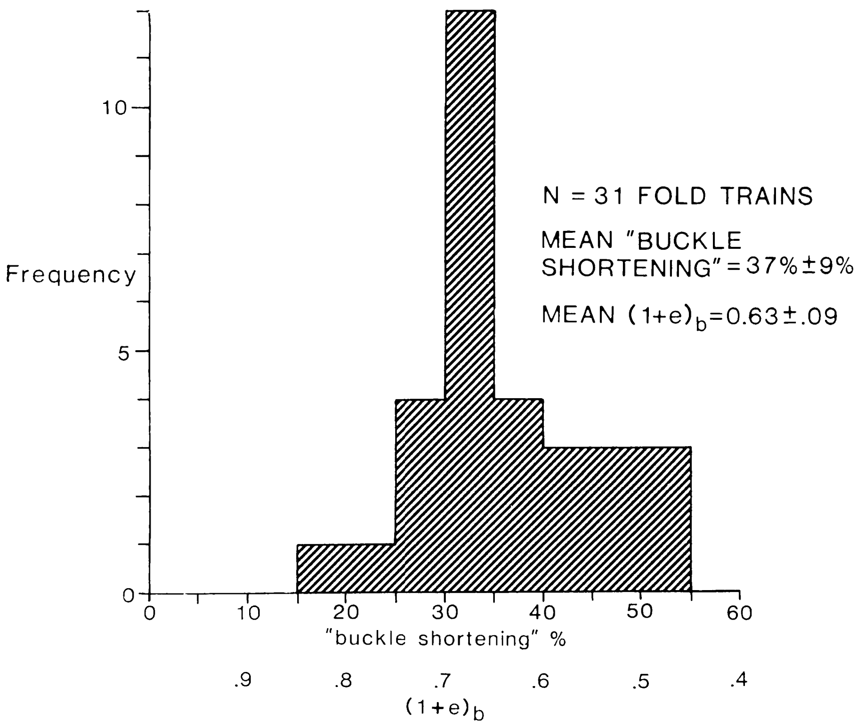

Fig. 7. Histogram of buckle shortening, the ratio of total arclength of a fold train to the straight-line distance between end points, for the 31 fold trains. This shortening is expressed (along the abscissa) both as a percentage and as values of buckling extension, $(1+e)_b$. See text for details.

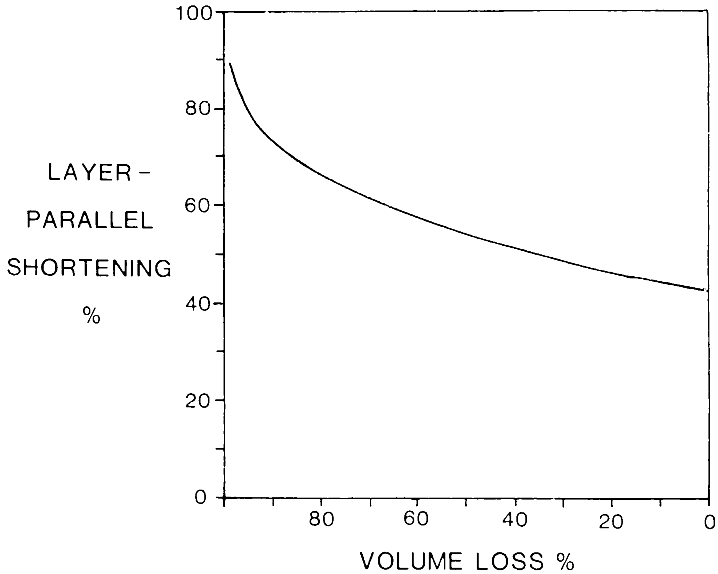

Fig. 8. Graph of the calculated layer-parallel shortening (expressed as a percentage) which took place in the quartz layers during the wavelength-selection (buckling) process as a function of volume loss assumed to have occurred during the deformation process. See text for details.

BUCKLING ANALYSIS

Buckling theory.—Early theoretical studies (Biot, 1961; Ramberg, 1961) showed that if an isolated linear viscous (Newtonian) layer embedded in a less viscous matrix is subject to compression parallel to the layer, the layer will buckle, and a particular wavelength (for a given thickness) will undergo the greatest amplification, leading to a "dominant wavelength/thickness ratio," L_d. For large viscosity contrasts (roughly $\mu_1/\mu_2 > 100$, where μ_1 is the viscosity of the layer and μ_2 the viscosity of the matrix), the dominant wavelength/thickness ratio is given by:

$$L_d = 2\pi\left(\frac{\mu_1}{6\mu_2}\right)^{1/3} \tag{2}$$

This relationship was verified experimentally, for large viscosity ratios (Biot, Ode, and Rover, 1961). For lower viscosity ratios, layer-parallel shortening during the buckling process becomes important. Sherwin and Chapple (1968) modified the buckling equation to account for layer-parallel shortening, T:

$$L_d = 2\pi\left[\left(\frac{\mu_1}{12\mu_2}\right)\left(\frac{T+1}{T^2}\right)\right]^{1/3} \tag{3}$$

The above is eq 6 of Sherwin and Chapple (1968) rewritten in the terminology of this paper. They also derived an expression for the amplification of the dominant wavelength (A_{max}) in terms of layer/matrix viscosity contrast and layer-parallel shortening. (The amplification is the ratio of final fold amplitude to amplitude of the initial perturbation in the layer.) Their eq 7 (Sherwin and Chapple, 1968) in the terminology of this paper is:

$$\ln A_{max} = \left(\frac{\mu_1}{\mu_2}\right)^{2/3} \left(\frac{3}{2T(T+1)}\right)^{1/3} \int_1^T \frac{d\tau}{1 + \frac{\tau^3}{T(T+1)}} \quad (4)$$

These expressions are perhaps best displayed in the graphical form of figure 9, illustrating the relationship between amplification of the

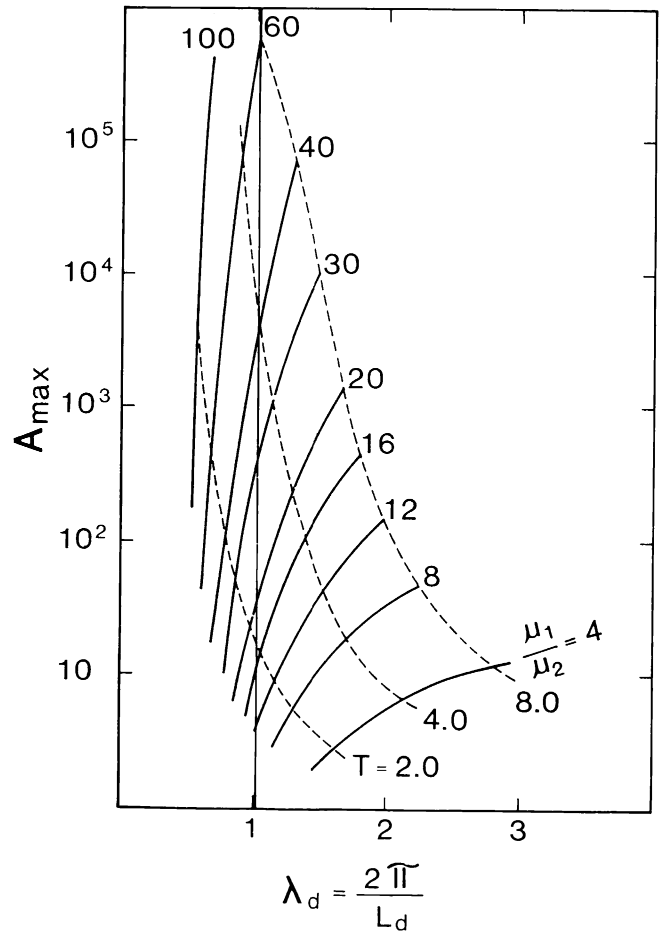

Fig. 9. Amplification of the dominant wavelength in terms of the dominant wavenumber ($\lambda_d = 2\pi/L_d$, in terminology of this paper), viscosity ratio of layer to matrix (μ_1/μ_2, solid contours), and layer-parallel shortening (T, dashed contours). Diagram after Sherwin and Chapple (1968, fig. 3). Vertical line at $\lambda_d = 1.01$ illustrates possible range of solutions for the dominant wavelength/thickness ratio result of this study ($L_d = 6.2$). A further constraint is placed on the interpretation by the calculated range of reasonable values of T. See text for details.

dominant wavelength, layer/matrix viscosity contrast, layer-parallel shortening, and the dominant wavelength/thickness ratio, here expressed as the dominant wavenumber ($\lambda_d = 2\pi/L_d$). Sherwin and Chapple (1968) suggested that, as layer-parallel shortening is impossible to measure in most cases, the amplification could be estimated, and then with measurements of fold geometry both layer/matrix viscosity contrast and layer-parallel shortening could be estimated.

Theoretical treatments of buckling of layers of non-Newtonian rheologies have been developed by Fletcher (1974) and Smith (1975, 1977, 1979). The theory of Sherwin and Chapple (1968) is the special case of the general buckling theory of Fletcher (1974), where the power-law exponent of the layer (n) is 1. For a given dominant wavelength/thickness ratio (L_d), the layer-parallel shortening (T) predicted by the theory decreases with increasing non-linearity of the layer (low values of T at high values of n). Using strain measurements of Groshong (1971, 1975) from within a folded limestone layer embedded in slates in the Valley and Ridge Province of Pennsylvania, Fletcher (1974) was able to show that the layer had behaved in a strongly non-linear manner during buckling ($3 \leqslant n \leqslant 12$). Using strain data from within a folded limestone layer in slate in the Canadian Rockies, Hudleston and Holst (1984) also concluded that folding had followed a non-linear flow law. In that case, linear-viscous theory could not account adequately for the data, as the measured value of layer-parallel shortening suggested an impossibly low amplification of the folds for the measured value of dominant wavelength/thickness ratio, according to linear-viscous theory.

In the general buckling theory additional variables are introduced so the data place less restrictive constraints on interpretations. Fletcher (1974) has shown that theoretical results are fairly insensitive to the power-law exponent of the matrix. If this is taken as unity we have as variables L_d, μ_1/μ_2 (the ratio of "effective" viscosity of layer to matrix), T, A_{max}, and n. Figure 10 (after Fletcher, 1974, fig. 5) shows the relationships between L_d, μ_1/μ_2 (in the parameter Q), T, and n for an amplification of 40.

Quartz rheology from experimental results.—Constraints on the interpretation of the fold and strain data from this study are also imposed by the results of rock deformation experiments on quartz aggregates. A reasonable body of data now exists as a result of such experiments, performed on different types of quartz aggregates at a variety of strain rates and environmental conditions. These results show that quartz aggregates follow a non-linear flow law during deformation. Most experimental values of the power-law exponent, n, are in the range from 1.8 to 2.8 (Koch, Christie, and George, 1980; Shelton and Tullis, 1981; Jaoul, Shelton, and Tullis, 1981; Hanson and Carter, 1982; Koch and Christie, 1982; Kronenberg and Tullis, 1984; Jaoul, Tullis, and Kronenberg, 1984; Kirby, 1985). Values as low as n = 1.2 have been observed using "wet" quartzite (Jaoul, Shelton, and Tullis, 1981).

Interpretation from the general buckling theory.—From the fold population we have a value of $\bar{L} = 6.2$. Using numerical simulation, Fletcher

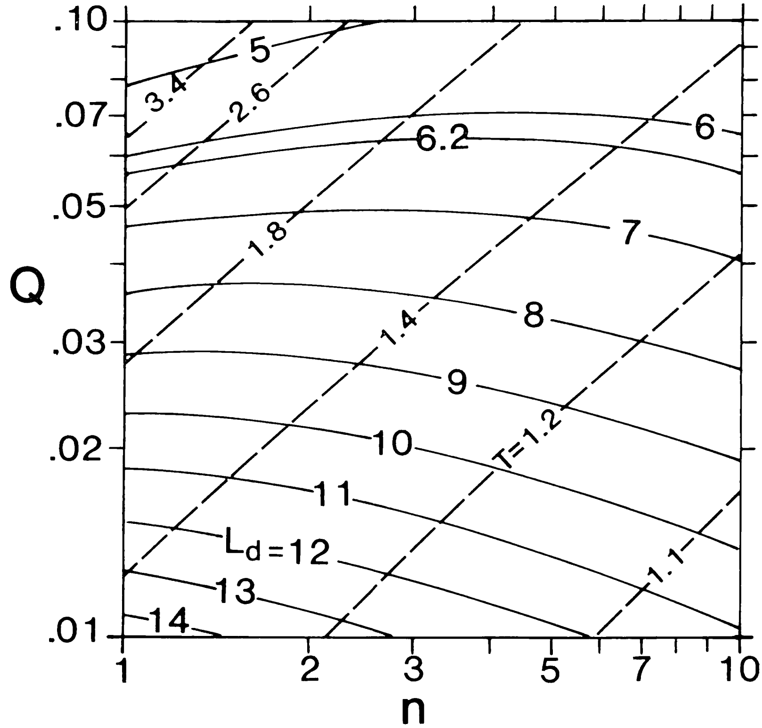

Fig. 10. Values of the rheological parameter Q $\left(Q = \frac{\mu_2}{\mu_1} n^{1/2}\right)$ expressed in terms of the power law exponent of the layer (n), the dominant wavelength/thickness ratio (L_d, solid contours), and layer-parallel shortening (T, dashed contours), for the condition $A_{max} = 40$ and a Newtonian matrix. Diagram after Fletcher (1974, fig. 5).

and Sherwin (1978) have shown that $\bar{L}$ is a valid approximation of L_d (the dominant wavelength/thickness ratio) for a particular spectrum of initial irregularities in the layer undergoing buckling. This spectrum, known as white roughness, is where all initial irregularities have the same limb dip, regardless of their wavelength. Such an initial amplitude spectrum is a good approximation of a number of natural surfaces, and Fletcher and Sherwin suggest it is a reasonable assumption for buckling analysis. We then have $L_d = 6.2$, and from the finite strain considerations we have a likely range of T values, $2.8 \leqslant T \leqslant 4$. We also have the experimental data that suggest n is in the range from just over 1 to 3. If we assume an amplification of 40 (a reasonable value), we can use figure 10 to interpret the data. On figure 10 the contour for a dominant wavelength/thickness ratio of 6.2 is drawn in. Here we see that for a value of $T = 2.8$, the predicted value of n is 1 (the intersection of L_d and $T = 2.8$ is the left edge of the diagram, the line $n = 1$).

If the case $n = 1$ is considered, we can use figure 9 (and eqs 3 and 4) to investigate the relationships of L_d, T, A_{max}, and μ_1/μ_2. For $L_d = 6.2$,

$\lambda_d = 1.01$. This line is drawn in figure 9. Exact solutions of eqs (3) and (4) yield, for $T = 2.8$, $\mu_1/\mu_2 = 24$, A_{max} just over 100, and for $T = 4$, $\mu_1/\mu_2 = 37$, $\log A_{max} = 3.53$. For the upper end of the likely shortening range these amplification values are unreasonably high, but the lower end of the shortening range yields reasonable values. However, the experimental results which show that quartz aggregates deform following non-linear flow laws suggest that $n = 1$ behavior is not likely.

We can use the general theory to investigate the relationships of the other variables if we allow n to vary from 1 to 3 at a value of $L_d = 6.2$. For an amplification of 40 we can use figure 10, which shows that as n varies from 1 to 3, T will vary from 2.8 to 1.7, below the range suggested from the finite strain analysis. Given the uncertainties in the finite strain arguments this is possible, but values of T below 2 are unlikely.

Other values of amplification also need to be considered. The data from the folds in the Little Falls Formation can perhaps best be interpreted with the aid of figure 11, showing the relationship of T and n for various values of A_{max}, and for the value $L_d = 6.2$. Here we see that for T to be greater than 2.8 and n near 2, amplifications are 300 or more.

No unique interpretation is possible, but certainly the values of n from experimental data (especially for "wet" quartz aggregates) and the low end of the range of T from the finite strain analysis do overlap at reasonable values of amplification. If we consider T values down to a value of 2, n in the range of 1 to 3, and amplifications from 20 to 300, many reasonable interpretations are possible. The most likely, given the constraints of the data, are for n in the range 1 to 2, T values near 2.8, and amplifications from 20 to 200.

Arclength/thickness frequency distributions and amplitude spectra.—An additional constraint may be placed on the interpretation when the dispersion, δ, of the frequency distribution of arclength/thickness data is considered. As mentioned previously, Fletcher and Sherwin (1978) showed that for an initial amplitude spectrum of white roughness, the dominant wavelength/thickness ratio (the one that has undergone the greatest amplification) is approximately equal to, and best estimated by, $\bar{L}$, the mean value of the arclength/thickness frequency distribution. Using numerical simulation, they also established the relationship between δ and the relative bandwidth of the amplitude spectrum that makes up the wave train, β. The relationship between the relative bandwidths of the initial amplitude spectrum and the amplification spectrum can be established for a given initial amplitude spectrum, allowing the relationship between the relative bandwidth of the amplification spectrum (β^*) and δ (the dispersion of the frequency distribution of arclength/thickness data) to be established. β^* is a function of power-law exponent of the layer, amplification, and layer/matrix viscosity contrast and thus provides an additional constraint of the interpretation of the data.

Fletcher and Sherwin (1978) evaluated dispersion of frequency distributions using half arclengths. The use of quarter arc segments in this study requires a correction in the calculation of the dispersion (Fletcher,

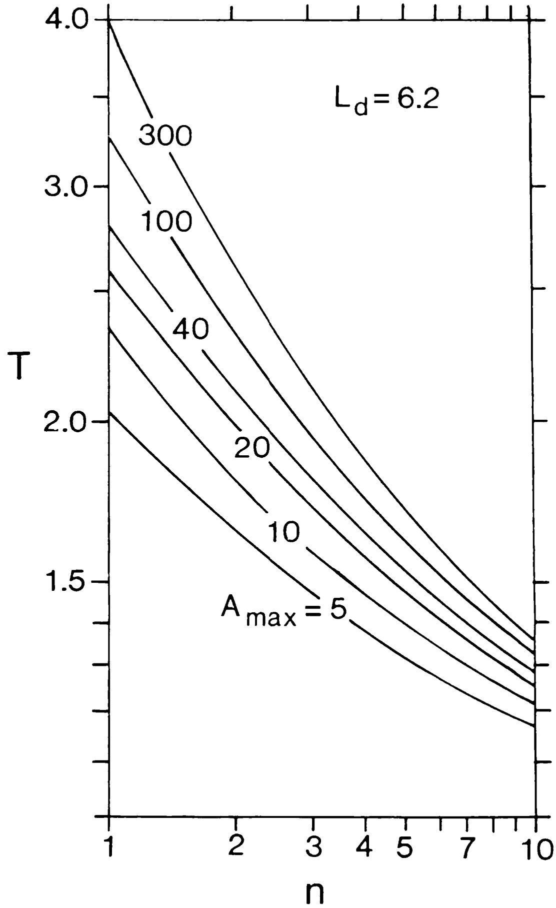

Fig. 11. The relationship of layer-parallel shortening during buckling (T) and power-law exponent of the layer (n), shown for various amplifications (A_{max}), and for the condition L_d = 6.2. Derived from the theoretical results of Fletcher (1974) and of the form of figure 9 of Hudleston and Holst (1984).

personal commun.). The dispersion of the frequency distribution of arc-length/thickness data from this study which should be applied to the correlation of δ and β^* in Fletcher and Sherwin (1978) is given by:

$$\delta = \sigma/(\sqrt{2})\,(\bar{L}) \tag{5}$$

The dispersion for this data is caused by natural variation and measurement error (Hudleston and Holst, 1984). Twenty-five measurements from a single quarter-arc fold segment gave the result $\bar{L} = 5.1$, $\sigma = 0.51$. Calculating the "true" variance (σ^2) as the difference between the variance for the fold population and the variance for the repeated measurements of the same quarter-arc fold segment, we find the "true" value of σ for the fold population to be 3.16, and the "true" dispersion to be 0.36. This gives a value of β^* of 1.18 (fig. 12).

As β^* is a function of amplification, layer/matrix viscosity ratio, and power law exponent, a unique interpretation of this value is not possible. However, it can be shown that considerations of arclength/thickness frequency distributions and amplitude spectra provide results consistent with the interpretation suggested earlier. For example, figure 13A shows the relationship of amplification and β^* for several values of layer/matrix viscosity ratio for the condition $n = 1$ (Newtonian behavior). Reasonable values of amplification (for example in the range 40-100) yield reasonable values of viscosity contrast for $\beta^* = 1.18$, the value for this study. At lower amplifications, higher viscosity contrasts are obtained. Figure 13B shows the same relationship for the case $n = 3$. Here, for the same range of amplification, the layer/matrix viscosity ratios are lower.

Alternative initial amplitude spectrum.—It is possible that the amplitude spectrum of initial irregularities in the layer was not that of white roughness. Fletcher and Sherwin (1978) consider a possible alternative where all initial surface irregularities have the same amplitude, thus longer wavelengths have lower initial limb dips. Such an initial spectrum was also considered by Hudleston and Holst (1984). In this case $\bar{L}$ does not provide an adequate approximation of L_d. Again using empirical results from numerical simulation, Fletcher and Sherwin (1978) establish the relationship between L_d (for this initial amplitude spectrum $L_d = L_m$, the wavelength/thickness ratio with the maximum amplitude in the wave train) and δ, the dispersion of the frequency distribution of arclength/thickness data. Using their result (Fletcher and Sherwin, 1978, fig. 5) and

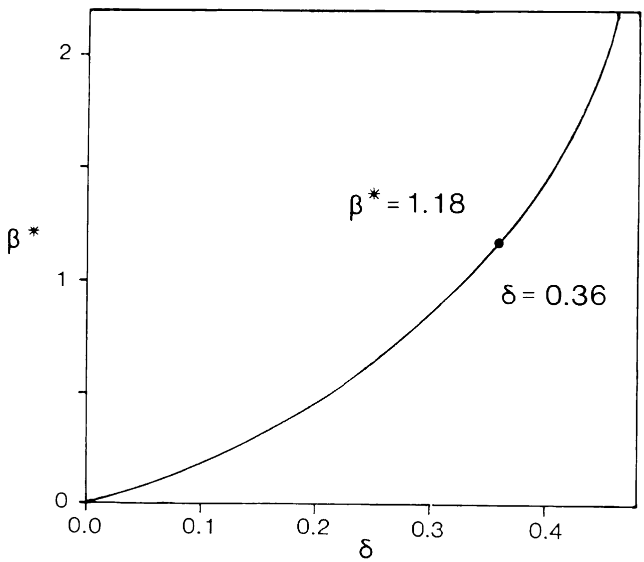

Fig. 12. The relationship of the relative bandwidth of the amplification spectrum (β^*) and dispersion (δ), with values pertinent to this study for an initial spectrum of white roughness. Diagram after Fletcher and Sherwin (1978, fig. 8).

A.

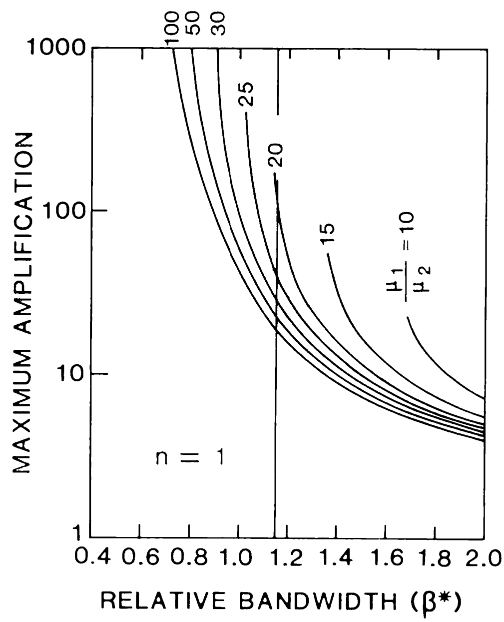

B.

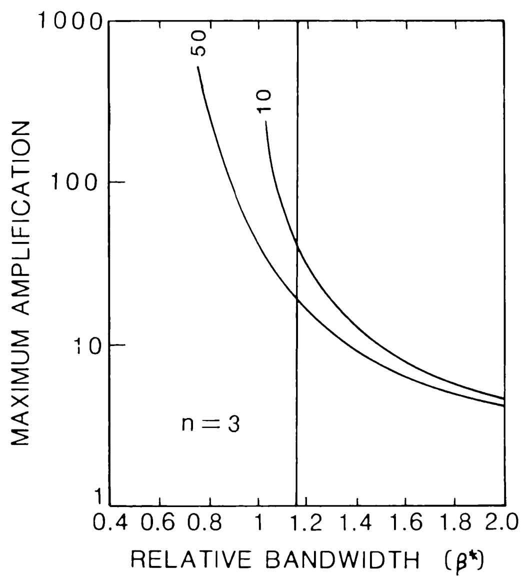

Fig. 13. The relationship of maximum amplification and relative bandwidth of the amplification spectrum at various viscosity contrasts between layer and matrix (μ_1/μ_2). Vertical lines are at $\beta^* = 1.18$, for the fold population in this study. (A) Newtonian layer (n = 1); (B) for a layer with power-law exponent n = 3. Diagrams after Fletcher and Sherwin (1978, fig. 9).

$\delta = 0.36$ from the data in this study, we find $\bar{L}/L_m = 0.79$. Since $L_m = L_d$ for this initial amplitude spectrum, and $\bar{L} = 6.2$ for this data set, we get an estimate of $L_d = 7.8$.

Again no unique interpretation is possible, but if the spectrum of initial irregularities was one of constant amplitude, higher amplifications or lower shortening values must be considered than in the case of an initial spectrum of white roughness.

Dispersion, δ, may again be used as a further constraint on interpretation. For an initial constant amplitude spectrum, the relative bandwidths of amplitude and amplification spectra are equal ($\beta = \beta^*$). Then for a dispersion $\delta = 0.36$ we find $\beta = \beta^* = 1.08$ (Fletcher and Sherwin, 1978, fig. 6). Again there is no unique interpretation of this result, but inspection of figure 13 shows that reasonable values of amplification and layer/matrix viscosity contrast are obtained.

Alternative growth mechanism.—Smith (1979) has discussed an alternative growth mechanism for folding of an extremely non-Newtonian layer which is quite different dynamically from classical buckling. Under these conditions, during layer-parallel compression any initial irregularities in an interface between two materials of contrasting rheology are not very effectively amplified. However, these initial irregularities produce a secondary flow within the layer which will deform the interface on the other side of the layer. For a material line sub-parallel to the interface, the most rapid deformation produced by the velocity distribution for this secondary flow within the layer occurs when the material line is located a distance from the interface equal to one-quarter of the wavelength of the irregularity in the interface producing the secondary flow. For this growth mechanism to be effective the deformation of the interfaces on each side of the layers (produced by motions caused by irregularities in the opposite interface) must reinforce each other. Hence this mechanism is most effective where the distance between interfaces is one-quarter of the wavelength of the initial irregularity producing the secondary flow. If there are initial irregularities of wavelength 4 times layer thickness, these will be most effectively amplified and will lead to fold growth. Smith (1979) thus suggests that this mechanism will always lead to a dominant arclength/thickness ratio equal to or slightly greater than 4. Using the arclength/thickness measurements from natural folds of Sherwin and Chapple (1968) and Johnson (1970), he suggests that L_d values of natural folds in the range 4 to 6 are common, and that the reason for this is that the layers behaved as extremely non-Newtonian materials, and this alternative growth mechanism was responsible for the development of the folds.

Smith does concede, however, that a large layer-parallel shortening accompanying the folding (by the classical buckling mechanism) of a Newtonian or nearly Newtonian layer will also lead to values of L_d in this range. He does suggest that if folds with low L_d values are as common as the (relatively few) existent data suggest, the alternative growth mechanism provides a more reasonable explanation for this than does the widespread occurrence of large values of layer-parallel shortening.

Considerations of non-plane strain.—Theoretical treatments of buckling assume plane strain. Clearly, the strain in the matrix is not plane strain, but if the volume loss was in the range of 10 to 30 percent, the strain is not far from plane (fig. 5). Within the layers there is no evidence (in the form of boudinage or pinch and swell) for large extension parallel with the fold axis (the direction of the Y axis), so strain within the layer is perhaps not far from plane strain. Hudleston and Holst (1984) pointed out that deviatoric stresses in the third dimension affect the buckling instability in power-law fluids. The net result is that stresses in the third dimension (parallel to the fold hinge) will tend to reduce the degree of non-linearity (reduce n) associated with the folding.

CONCLUSIONS

The folds that have developed in quartz layers embedded in the graywacke-slate sequence of the Little Falls Formation show characteristics typical of folds developed by buckling. A preference for a dominant arclength/thickness ratio exists, and the folds are of parallel or sub-parallel geometry. It seems fairly certain that these quartz layers have suffered the same deformation history as the matrix, and thus the strain determinations from the matrix do indicate that layer-parallel shortening within the layer played an important role during the buckling process. This, along with experimental values of n in the range 1.8 to 2.8 for quartz aggregates, indicates that the secondary-flow growth mechanism for highly non-linear materials (Smith, 1979) was not the growth mechanism responsible for the folds. Instead, classical buckling and wavelength selection were responsible for the folding and present fold geometry. The fold geometry and strain data may be interpreted with the aid of buckling theory, although no unique interpretation is possible. The most likely values of T are near 2.8, with amplifications from 20 to 200, μ_1/μ_2 in the range 20 to 40, and n between 1 and 2.

ACKNOWLEDGMENTS

This research was supported by National Science Foundation Grant EAR 8420089. Daniel Holm assisted in collection of fold geometry data. Mike Ellis made helpful suggestions on an early draft of the paper. The comments of Ray Fletcher and discussions with Peter Hudleston are gratefully acknowledged.

REFERENCES

Agostino, P. N., 1971, Theoretical and experimental investigations on ptygmatic structures: Geol. Soc. America Bull., v. 82, p. 2651-2660.

Biot, M. A., 1961, Theory of folding of stratified viscoelastic media and its implications in tectonics and orogenesis: Geol. Soc. America Bull., v. 72, p. 1595-1620.

Biot, M. A., Ode, H., and Roever, W. L., 1961, Experimental verification of the theory of folding of stratified viscoelastic media: Geol. Soc. America Bull., v. 72, p. 1621-1632.

Chandler, V. W., Nordstrand, E., and Anderson, S., 1984, Shaded relief aeromagnetic anomaly map of northeastern and east-central Minnesota: Minnesota Geol. Survey, Misc. Map Ser., Map M-53.

Chapple, W. M., 1968, A mathematical theory of finite-amplitude rock-folding: Geol. Soc. America Bull., v. 79, p. 47-68.

Cobbold, P. R., 1975, Fold propagation in single embedded layers: Tectonophysics, v. 27, p. 333-351.

Dieterich, J. H., 1969, Origin of cleavage in folded rocks: Am. Jour. Sci., v. 267, p. 155-165.

Dunnet, D., and Siddans, A. W. B., 1971, Non-random sedimentary fabrics and their modification by strain: Tectonophysics, v. 12, p. 307-325.

Elliott, D., 1970, Determination of finite strain and initial shape from deformed elliptical objects: Geol. Soc. America Bull., v. 81, p. 2221-2236.

Fletcher, R. C., 1974, Wavelength selection in the folding of a single layer with power-law rheology: Am. Jour. Sci., v. 274, p. 1029-1043.

Fletcher, R. C., and Sherwin, J.-A., 1978, Arc lengths of single layer folds: a discussion of the comparison between theory and observation: Am. Jour. Sci., v. 278, p. 1085-1098.

Groshong, R. H., Jr., 1971, Strain in natural single-layer folds [abs.]: Am. Geophys. Union Trans., v. 52, p. 345.

——— 1975, Strain, fractures, and pressure solution in natural single-layer folds: Geol. Soc. America Bull., v. 86, p. 1363-1376.

Hanson, F. D., and Carter, N. L., 1982, Creep of selected crustal rocks at 1000 MPa [abs.]: Am. Geophys. Union Trans., v. 63, p. 437.

Holst, T. B., 1982a, Evidence for multiple deformation during the Penokean orogeny in the middle Precambrian Thomson Formation, Minnesota: Canadian Jour. Earth Sci., v. 19, p. 2043-2047.

——— 1982b, The role of initial fabric on strain determination from deformed ellipsoidal objects: Tectonophysics, v. 82, p. 329-350.

——— 1984, Evidence for nappe development during the early Proterozoic Penokean orogeny, Minnesota: Geology, v. 12, p. 135-138.

——— 1985a, Implications of a large flattening strain for the origin of a bedding-parallel foliation in the early Proterozoic Thomson Formation, Minnesota: Jour. Structural Geology, v. 7, p. 375-383.

——— 1985b, Reply to comment on "Evidence for nappe development during the early Proterozoic Penokean orogeny, Minnesota": Geology, v. 13, p. 444-445.

Hossack, J. R., 1968, Pebble deformation and thrusting in the Bygdin area (southern Norway): Tectonophysics, v. 5, p. 315-339.

Hudleston, P. J., 1973a, An analysis of single layer folds developed experimentally in viscous media: Tectonophysics, v. 16, p. 189-214.

——— 1973b, The analysis and interpretation of minor folds developed in the Moine rocks of Monar, Scotland: Tectonophysics, v. 16, p. 89-132.

Hudleston, P. J., and Holst, T. B., 1984, Strain analysis and fold shape in a limestone layer and implications for layer rheology: Tectonophysics, v. 106, p. 321-347.

Hudleston, P. J., and Stephansson, O., 1973, Layer shortening and fold shape development in the buckling of single layers: Tectonophysics, v. 17, p. 299-321.

Jaoul, O., Shelton, G., and Tullis, J., 1981, Quartzite deformation as a function of water at 15 kb: Preliminary results [abs.]: Am. Geophys. Union Trans., v. 62, p. 396.

Jaoul, O., Tullis, J., and Kronenberg, A. K., 1984, The effect of varying water contents on the creep behavior of Heavitree Quartzite: Jour. Geophys. Research, v. 89, p. 4298-4312.

Johnson, A. M., 1970, Physical Processes in Geology: San Francisco, Freeman, Cooper, and Co., 577 p.

Kirby, S. H., 1985, Rock mechanics observations pertinent to the rheology of the continental lithosphere and the localization of strain along shear zones: Tectonophysics, v. 119, p. 1-27.

Koch, P. S., and Christie, J. M., 1982, High-temperature flow of Arkansas Novaculite in the α-quartz field [abs.]: Am. Geophys. Union Trans., v. 63, p. 1095.

Koch, P. S., Christie, J. M., and George, R. P., 1980, Flow law of "wet" quartzite in the α-quartz field [abs.]: Am. Geophys. Union Trans., v. 61, p. 376.

Kronenberg, A. K., and Tullis, J., 1984, Flow strengths of quartz aggregates: Grain size and pressure effects due to hydolytic weakening: Jour. Geophys. Research, v. 89, p. 4281-4297.

Manz, R., and Wickham, J., 1978, Experimental analysis of folding in simple shear: Tectonophysics, v. 44, p. 79-90.

Morey, G. B., 1978, Lower and middle Precambrian stratigraphic nomenclature for east-central Minnesota: Minnesota Geol. Survey Rept. Inv. RI-21, 52 p.

——— 1980, Field Trip Guidebook for the Precambrian Geology of East-Central Minnesota: Minnesota Geol. Survey Guidebook Ser. 12, 38 p.

Morey, G. B., and Ojakangas, R. W., 1970, Sedimentology of the middle Precambrian Thomson Formation, east-central Minnesota: Minnesota Geol. Survey Rept. Inv. RI-13, 32 p.

Morey, G. B., Sims, P. K., Cannon, W. F., Mudrey, M. G., Jr., and Southwick, D. L., 1982, Geologic Map of the Lake Superior Region; Minnesota, Wisconsin, and Northern Michigan: Minnesota Geol. Survey State Map Ser. S-13.

Morey, G. B., and Southwick, D. L., 1984, Early Proterozoic Geology of east-central Minnesota — A Review and Reappraisal: Inst. on Lake Superior Geology, Proc., v. 30, p. 35-36.

Nadai, A., 1963, Theory of Flow and Fracture of Solids — Engineering Societies Monographs: New York, McGraw-Hill Book Co., 705 p.

Neurath, C., and Smith, R. B., 1982, The effect of material properties on growth rates of folding and boudinage: experiments with wax models: Jour. Structural Geology, v. 4, p. 215-229.

Parrish, D. K., 1973, A nonlinear finite element fold model: Am. Jour. Sci., v. 273, p. 318-334.

Ramberg, H., 1961, Contact strain and folding instability of a multilayered body under compression: Geol. Rundschau., v. 51, p. 405-439.

Ramsay, J. G., 1967, Folding and Fracturing of Rocks: New York, McGraw-Hill Book Co., 568 p.

Ramsay, J. G., and Wood, D. S., 1973, The geometric effects of volume change during deformation processes: Tectonophysics, v. 16, p. 263-277.

Schwartz, G. M., 1942, Concretions of the Thomson Formation, Minnesota: Am. Jour. Sci., v. 240, p. 491-499.

Shelton, G., and Tullis, J., 1981, Experimental flow laws for crustal rocks [abs.]: Am. Geophys. Union Trans., v. 62, p. 396.

Sherwin, J.-A., and Chapple, W. M., 1968, Wavelengths of single layer folds: a comparison between theory and observation: Am. Jour. Sci., v. 266, p. 167-179.

Smith, R. B., 1975, Unified theory of the onset of folding, boudinage, and mullion structure: Geol. Soc. America Bull., v. 86, p. 1601-1609.

——— 1977, Formation of folds, boudinage, and mullions in non-Newtonian materials: Geol. Soc. America Bull., v. 88, p. 312-320.

——— 1979, The folding of a strongly non-Newtonian layer: Am. Jour. Sci., v. 279, p. 272-287.

Van Schmus, W. R., 1976, Early and middle Proterozoic history of the Great Lakes area, North America: Royal Soc. Philos. Trans., v. A280, p. 605-628.

——— 1980, Chronology of igneous rocks associated with the Penokean orogeny in Wisconsin, *in* Morey, G. B., and Hanson, G. N., eds., Selected studies of Archean gneisses and lower Proterozoic rocks, southern Canadian Shield: Geol. Soc. America Spec. Paper 182, p. 159-168.

Wood, D. S., 1974, Current views of the development of slaty cleavage: Ann. Rev. Earth Planetary Sci., v. 2, p. 1-35.

Wright, T. O., and Platt, L. B., 1982, Pressure dissolution and cleavage in the Martinsburg Shale: Am. Jour. Sci., v. 282, p. 122-135.